

Protein substrates engage the lumen of O-GlcNAc transferase's tetratricopeptide repeat domain in different ways

Cassandra M. Joiner[1]*, Forrest A. Hammel[1][2], John Janetzko[1][3], Suzanne Walker[1]*

Author Address

[1] Department of Microbiology, Harvard Medical School, 4 Blackfan Circle, Boston, MA 02115, USA

[2] Program in Chemical Biology, Harvard University, 12 Oxford Street, Cambridge, MA 02138, USA

[3] Department of Chemistry and Chemical Biology, Harvard University, 12 Oxford Street, Cambridge, MA 02138, USA

*Corresponding authors.

E-mails: Suzanne_walker@hms.harvard.edu

Joiner1@stolaf.edu

Supplemental Table S1-S7	S2
Supplemental Figures S1-S6	S5
General Methods	S11
Tables of Plasmids	S11
Tables of Primers	S11
Table of Gene Blocks	S12
Construction of pET24-8XHIS-HRV3C-ncOGT variants	S12
Construction of TAB1 S395A and CAMKIV S189A variants	S13
Bacterial expression and purification of pET24-8XHIS-HRV3C-ncOGT variants	S13
<i>In vitro</i> glycosylation of HeLa extracts by ncOGT variants	S13
Bacterial expression and purification of OGT substrates	S14
<i>In vitro</i> glycosylation of OGT substrates by ncOGT variants	S14
<i>In vitro</i> turnover assay of TAB1 glycosylation by ncOGT variants	S14
<i>In vitro</i> time-dependent glycosylation of CAMKIV by ncOGT variants	S15
References	S15

Supplemental Table S1. OGT Asparagine Ladder Conservation Table

Residue	% Conservation per amino acid	
	N	Next highest cons. residues
N458	88.9	2.7 - S
N424	96.3	1.0 – S, 1.0 - A
N390	95.6	1.7 - S
N356	95.9	1.7 - S
N322	95.9	1.0 - D
N288	94.2	1.7 - D
N254	91.8	1.7 - S, 1.7 - K
N220	90.7	3.2 - S
N186	93.1	3.0 - A
N155	82.7	4.1 - D
N118	83.6	7.6 - L
N84	87.6	3.6 - S

Conservation scores determined for OGT's TPR domain using the 1W3B PDB file and ConSurf Server.¹⁻³ 150 sequence homologs were compared.

Supplemental Table S2. OGT Aspartate Ladder Conservation Table

Residue	% Conservation per amino acid	
	D	Next highest cons. residues
D454	54.5	33.8 - E
D420	53.2	38.1 - E
D386	81.8	9.8 - E
D318	49.5	11.9 - E
D284	55.9	34.8 - E
D216	80.6	13.6 - E
D152*	45.9	48.1 - N
D114	85.8	4.4 - E

* Position 152 can be either an aspartate (D – 45.9% conservation) or asparagine (N- 48.1% conservation). Conservation scores determined for OGT's TPR domain using the 1W3B PDB file and ConSurf Server.¹⁻³ 150 sequence homologs were compared.

Supplemental Table S3. Quantification of *in vitro* glycosylation of purified substrates by OGT TPR truncation mutants

OGT constructs	TAB1 (1-504) Glycosylation Signal (Fold change compared to OGT WT)			TAB1 (1-402) Glycosylation Signal (Fold change compared to OGT WT)			CARM1 Glycosylation Signal (Fold change compared to OGT WT)			CAMKIV Glycosylation Signal (Fold change compared to OGT WT)		
	Rep 1	Rep 2	Avg	Rep 1	Rep 2	Avg	Rep 1	Rep 2	Avg	Rep 1	Rep 2	Avg
OGT WT	1.0	1.0	1.00	1.0	1.0	1.00	1.0	1.0	1.00	1.0	1.0	1.00
OGT Δ1	0.1	0.1	0.10	1.1	1.0	1.05	0.8	0.8	0.80	0.2	0.5	0.35
OGT Δ2	0.0	0.1	0.05	1.0	1.0	1.00	0.7	0.7	0.70	0.5	0.5	0.50
OGT Δ3	0.0	0.1	0.05	1.4	1.0	1.20	0.7	0.8	0.75	1.7	1.2	1.45
OGT Δ4	0.1	0.2	0.15	1.3	1.0	1.15	0.7	0.9	0.80	2.4	2.0	2.20
OGT Δ5	0.1	0.4	0.25	1.4	1.1	1.25	0.8	1.0	0.90	2.8	2.5	2.65
OGT Δ6	0.1	0.3	0.20	1.5	1.0	1.25	0.9	1.0	0.95	2.0	1.8	1.90

Supplemental Table S4. Quantification of *in vitro* glycosylation of purified substrates by OGT N5A mutants

OGT constructs	TAB1 (1-504) Glycosylation Signal (Fold change compared to OGT WT)			TAB1 (1-402) Glycosylation Signal (Fold change compared to OGT WT)			CARM1 Glycosylation Signal (Fold change compared to OGT WT)			CAMKIV Glycosylation Signal (Fold change compared to OGT WT)		
	Rep 1	Rep 2	Avg	Rep 1	Rep 2	Avg	Rep 1	Rep 2	Avg	Rep 1	Rep 2	Avg
OGT WT	1.0	1.0	1.00	1.0	1.0	1.00	1.0	1.0	1.00	1.0	1.0	1.00
OGT N5A _{prox}	0.1	0.1	0.10	1.1	1.0	1.05	1.0	1.0	1.00	0.4	0.4	0.40
OGT N5A _{med}	0.1	0.1	0.10	1.1	1.0	1.05	1.0	1.0	1.00	0.5	0.5	0.50
OGT N5A _{dist}	0.2	0.2	0.20	1.1	0.9	1.00	0.9	0.9	0.90	1.1	1.1	1.10

Supplemental Table S5. Quantification of *in vitro* glycosylation of purified substrates by OGT D2A mutants

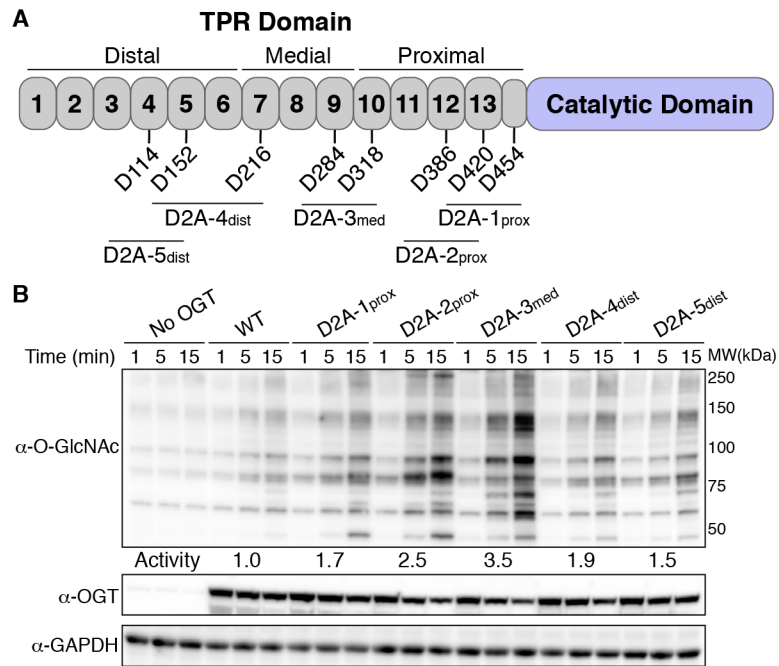
OGT constructs	TAB1 (1-504) Glycosylation Signal (Fold change compared to OGT WT)			TAB1 (1-402) Glycosylation Signal (Fold change compared to OGT WT)			CARM1 Glycosylation Signal (Fold change compared to OGT WT)			CAMKIV Glycosylation Signal (Fold change compared to OGT WT)		
	Rep 1	Rep 2	Avg	Rep 1	Rep 2	Avg	Rep 1	Rep 2	Avg	Rep 1	Rep 2	Avg
OGT WT	1.0	1.0	1.00	1.0	1.0	1.00	1.0	1.0	1.00	1.0	1.0	1.00
OGT D2A- _{1prox}	2.2	2.4	2.30	1.2	0.9	1.05	0.9	1.0	0.95	1.8	1.7	1.75
OGT D2A- _{2prox}	2.2	2.5	2.35	1.1	0.9	1.00	1.4	1.3	1.35	2.7	2.9	2.80
OGT D2A- _{3med}	2.0	2.3	2.15	1.1	1.0	1.05	1.3	1.5	1.40	8.1	7.8	7.95
OGT D2A- _{4dist}	0.9	0.9	0.90	1.1	1.0	1.05	1.2	1.3	1.25	3.1	3.1	3.10
OGT D2A- _{5dist}	0.8	0.7	0.75	1.1	1.0	1.05	1.6	1.4	1.50	3.1	3.1	3.10

Supplemental Table S6. Quantification of *in vitro* turnover of TAB1 glycosylation by OGT WT and D2A-2_{prox}

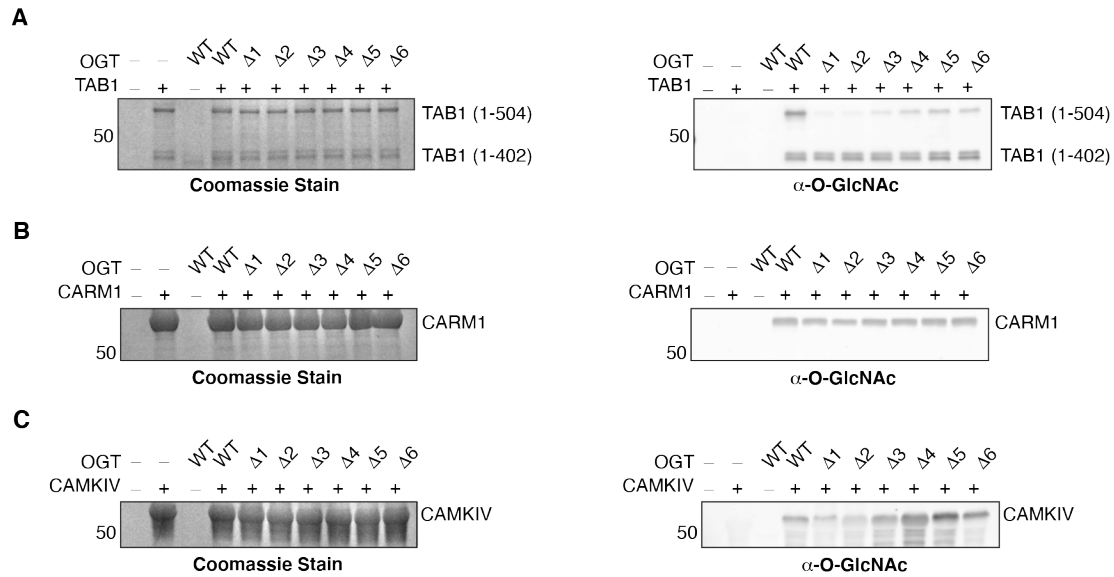
Time (min)	OGT WT_Rep 1 (densitometry)	OGT WT_Rep 2 (densitometry)	OGT D2A- 2prox_Rep1 (densitometry)	OGT D2A- 2prox_Rep2 (densitometry)
0.0	2.2	4.5	2.3	2.2
1.0	7.5	5.9	43.8	37.7
2.5	16.1	10.4	68.9	62.9
5.0	25.0	20.8	86.3	84.1
10.0	41.0	32.9	92.7	97.7
15.0	60.1	48.0	95.0	104.3
20.0	63.0	55.5	97.1	107.0
30.0	62.1	64.2	97.9	98.1

Supplemental Table S7. Quantification of *in vitro* turnover of TAB1 S395A glycosylation by OGT WT and D2A-2_{prox}

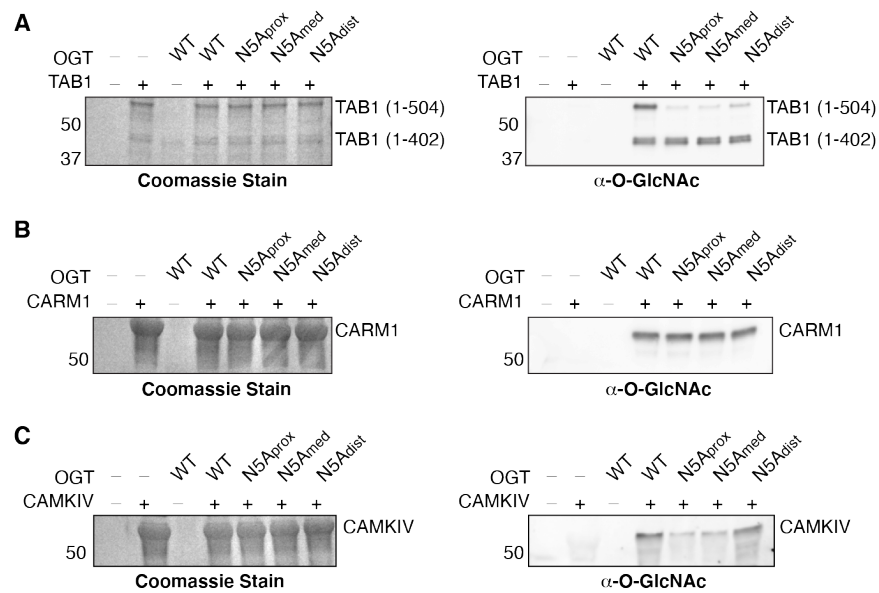
Time (min)	OGT WT_Rep 1 (densitometry)	OGT WT_Rep 2 (densitometry)	OGT D2A- 2prox_Rep1 (densitometry)	OGT D2A- 2prox_Rep2 (densitometry)
0.0	0.8	1.2	0.0	0.0
1.0	0.8	1.2	0.0	0.1
5.0	0.8	1.6	2.3	2.0
10.0	0.9	2.0	7.9	4.0
15.0	1.8	1.8	6.7	5.9
20.0	2.0	1.2	7.1	6.8
30.0	3.5	1.2	9.1	7.9



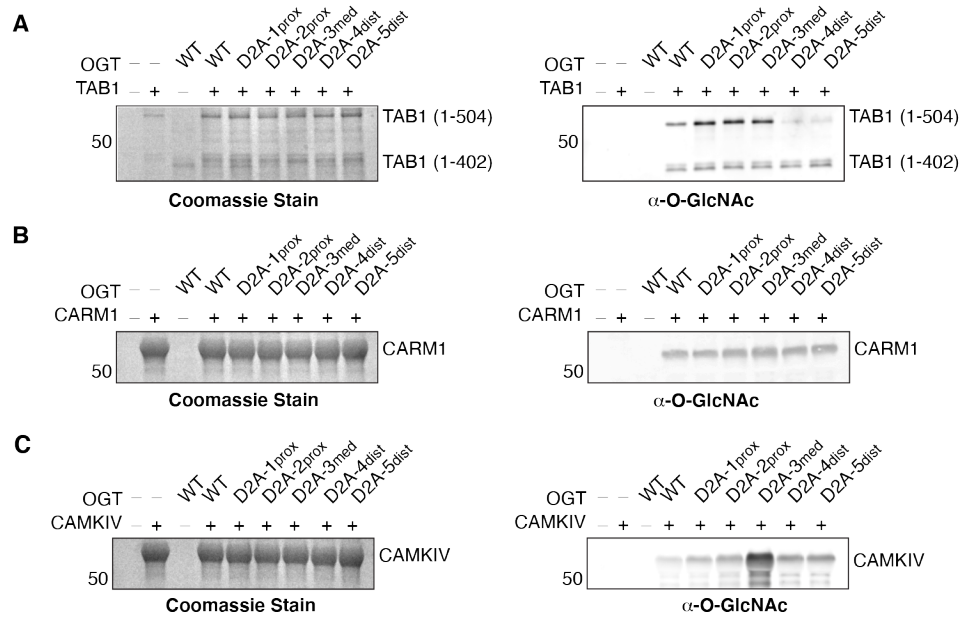
Supplemental Figure S1. Aspartate ladder differentially regulates global glycosylation of HeLa extracts. (A) Cartoon schematic of OGT D2A mutant constructs. (B) Glycosylation of HeLa extracts shows differential increases in glycosylation for D2A mutants with largest increases for D2A-2 and D2A-3. Representative blot for two independent experiments. See methods for relative glycosylation activity calculations.



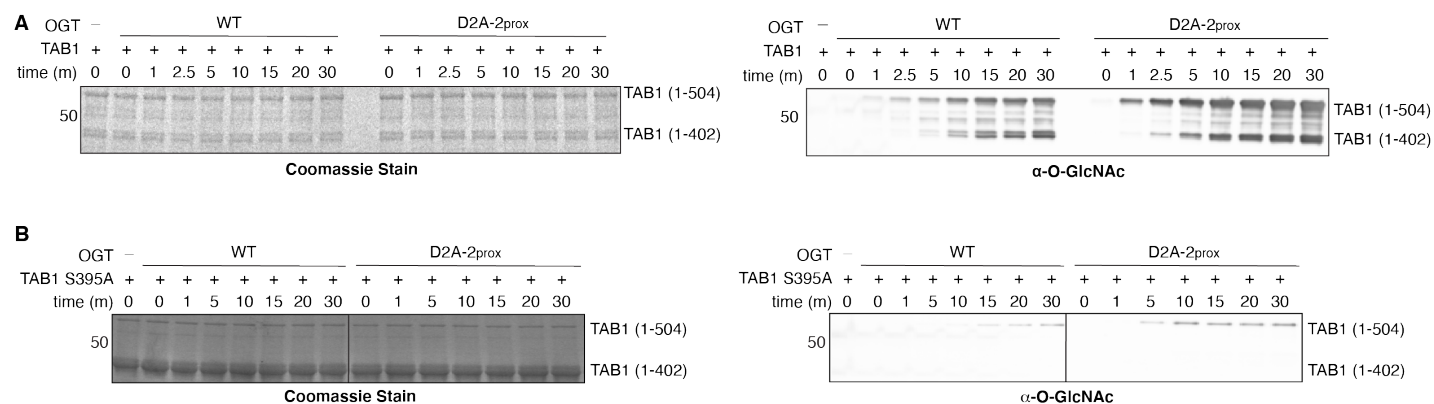
Supplemental Figure S2. SDS-PAGE gels and western blots of *in vitro* glycosylation of OGT substrates by OGT TPR truncation variants. A) *In vitro* glycosylation of TAB1 by TPR truncation mutants. B) *In vitro* glycosylation of CARM1 by TPR truncation mutants. C) *In vitro* glycosylation of CAMKIV by TPR truncation mutants. Glycosylation assays were run for 90 minutes. All SDS-PAGE gels were stained with Instant Blue Coomassie stain and western blots were visualized using the pan O-GlcNAc antibody CTD110.6. Representative gels and blots are shown for two independent experiments for each data set.



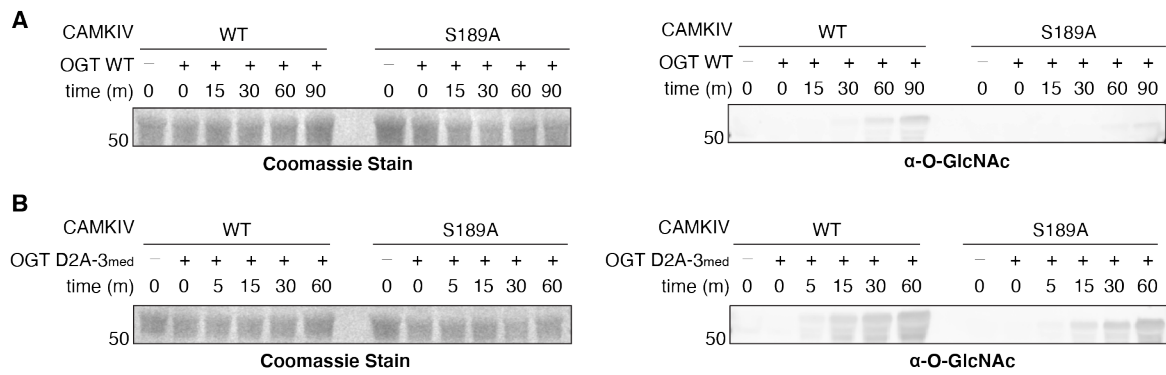
Supplemental Figure S3. SDS-PAGE gels and western blots of *in vitro* glycosylation of OGT substrates by OGT asparagine ladder variants. A) *In vitro* glycosylation of TAB1 by N5A mutants. B) *In vitro* glycosylation of CARM1 by N5A mutants. C) *In vitro* glycosylation of CAMKIV by N5A mutants. Glycosylation assays were run for 90 minutes. All SDS-PAGE gels were stained with Instant Blue Coomassie stain and western blots were visualized using the pan O-GlcNAc antibody CTD110.6. Representative gels and blots are shown for two independent experiments for each data set.



Supplemental Figure S4. Full length SDS-PAGE gels and western blots of *in vitro* glycosylation of OGT substrates by OGT aspartate ladder variants. A) *In vitro* glycosylation of TAB1 by D2A mutants. B) *In vitro* glycosylation of CARM1 by D2A mutants. C) *In vitro* glycosylation of CAMKIV by D2A mutants. Glycosylation assays were run for 90 minutes. All SDS-PAGE gels were stained with Instant Blue Coomassie stain and western blots were visualized using the pan O-GlcNAc antibody CTD110.6. Representative gels and blots are shown for two independent experiments for each data set.



Supplemental Figure S5. SDS-PAGE gels and western blots of *in vitro* glycosylation of TAB1 WT and S395A by OGT variants. Time-dependent *in vitro* glycosylation of A) TAB1 WT and B) TAB1 S395A by OGT WT and D2A-2_{prox}. Western blot and gel images in panel A and B were acquired under identical conditions. Representative gels and blots are shown for two independent experiments.



Supplemental Figure S6. Time dependent *in vitro* glycosylation of CAMKIV WT and S189A by OGT variants. A) Time-dependent *in vitro* glycosylation of CAMKIV WT and S189A by OGT WT shows that S189 is the major glycosite for CAMKIV. Max glycosylation of CAMKIV WT by wildtype OGT is seen at 90 min. B) Time-dependent *in vitro* glycosylation of CAMKIV WT and S189A by OGT D2A-3_{med} shows glycosylation of CAMKIV WT as early as 5 minutes. D2A-3_{med} shows increased glycosylation of CAMKIV compared to wildtype OGT. Western blots in panels A and B were imaged at the same time under identical conditions. Representative blots are shown for two independent experiments.

General Methods

All primers and gene blocks were purchased from Integrated DNA Technologies (IDT) and all isolated plasmid were verified by sequencing by the Dana-Farber/Harvard Cancer Center DNA Resource Core (Boston, MA).

Table of Plasmids

Plasmids	Function	Reference
pET24b-8XHIS-HRV3C-ncOGT WT	Expresses 8XHIS-HRV3C-ncOGT (1-1036)	6
pET24b-8XHIS-HRV3C-ncOGT N5A _{prox}	Expresses 8XHIS-HRV3C-ncOGT (1-1036) with GCA codon replacing N322, N356, N390, N424, and N458	7,8
pET24b-8XHIS-HRV3C-ncOGT N5A _{med}	Expresses 8XHIS-HRV3C-ncOGT (1-1036) with GCA codon replacing N186, N220, N254, N288, and N322	This study
pET24b-8XHIS-HRV3C-ncOGT N5A _{dist}	Expresses 8XHIS-HRV3C-ncOGT (1-1036) with GCA codon replacing N84, N118, N155, N186, and N220	This study
pET24b-8XHIS-HRV3C-ncOGT D420A/D454A (D2A-1 _{prox})	Expresses 8XHIS-HRV3C-ncOGT (1-1036) with GCA codon replacing the existing amino acids	9
pET24b-8XHIS-HRV3C-ncOGT D386A/D420A (D2A-2 _{prox})	Expresses 8XHIS-HRV3C-ncOGT (1-1036) with GCA codon replacing the existing amino acids	9
pET24b-8XHIS-HRV3C-ncOGT D284A/D318A (D2A-3 _{med})	Expresses 8XHIS-HRV3C-ncOGT (1-1036) with GCA codon replacing the existing amino acids	This study
pET24b-8XHIS-HRV3C-ncOGT D152A/D216A (D2A-4 _{dist})	Expresses 8XHIS-HRV3C-ncOGT (1-1036) with GCA codon replacing the existing amino acids	This study
pET24b-8XHIS-HRV3C-ncOGT D114A/D152A (D2A-5 _{dist})	Expresses 8XHIS-HRV3C-ncOGT (1-1036) with GCA codon replacing the existing amino acids	This study
pET24b-8XHIS-HRV3C-ncOGT D284A/D386A/D420A/D454A (D4A)	Expresses 8XHIS-HRV3C-ncOGT (1-1036) with GCA codon replacing the existing amino acids	This study
pET24b-8XHIS-HRV3C-ncOGT Δ 1	Expresses 8XHIS-HRV3C-ncOGT (323-1036) containing 4.5 TPRs (TPRs 10-13.5)	5
pET24b-8XHIS-HRV3C-ncOGT Δ 2	Expresses 8XHIS-HRV3C-ncOGT (289-1036) containing 5.5 TPRs (TPRs 9-13.5)	This study
pET24b-8XHIS-HRV3C-ncOGT Δ 3	Expresses 8XHIS-HRV3C-ncOGT (238-1036) containing 6.5 TPRs (TPRs 8-13.5)	This study
pET24b-8XHIS-HRV3C-ncOGT Δ 4	Expresses 8XHIS-HRV3C-ncOGT (221-1036) containing 7.5 TPRs (TPRs 7-13.5)	This study
pET24b-8XHIS-HRV3C-ncOGT Δ 5	Expresses 8XHIS-HRV3C-ncOGT (203-1036) containing 8.0 TPRs (TPRs 6.5-13.5)	This study
pET24b-8XHIS-HRV3C-ncOGT Δ 6	Expresses 8XHIS-HRV3C-ncOGT (169-1036) containing 9.0 TPRs (TPRs 5.5-13.5)	This study
pET28a-CARM1	Expresses polyhistidine-tagged CARM1	4
pET28a-CAMKIV	Expresses polyhistidine-tagged CAMKIV	4
pET28a-TAB1	Expresses polyhistidine-tagged TAB1	4
pET28a-TAB1 S395A	Expresses polyhistidine-tagged TAB1 with GCA codon replacing S395.	This study
pET28a-CAMKIV S189A	Expresses polyhistidine-tagged CAMKIV with GCA codon replacing S189	This study

Table of Primers

Primer ID	Sequence
ncOGT N5A-2 FOR	5' - GCAGACCAAGCAACAGCGAAGTTCGGCTGGGTTTCG – 3'
ncOGT N5A-2 REV	5' – GGCTAACATCAAACGTGAACAGGGTAACATCGAAGAAGCTG – 3'
ncOGT N5A-3 FOR	5' – GAGTAAGCTTCAGCCAGCAGCGGGTTCTGTTTGATAGC – 3'
ncOGT N5A-3 REV	5' – CACTGGGTAACGTTCTGAAAGAAGCTCGTATCTTCGACCGTGC – 3'

ncOGT D318A FOR	5' – GTGCCCCGACCCACGCT GC ATCTCTGAACAACCTGG – 3'
ncOGT D318A REV	5' – CCAGGTTGTTTCAGAGAT GC AGCGTGGGTCGGGCAC – 3'
ncOGT D284A FOR	5' – CAGCCGCACTTTCCAG GC AGCTTACTGCAACCTGG – 3'
ncOGT D284A REV	5' – CCAGGTTGCAGTAAGCT GC TGGAAAGTGCGGCTG – 3'
ncOGT D216A FOR	5' – GGACCCGAACCTCCT GC AGCTTACATCAACCTGG – 3'
ncOGT D216A REV	5' – CCAGGTTGATGTAAGCT GC CCAGGAAGTTCGGGTCC – 3'
ncOGT D152A FOR	5' – CGTTCGTTCT GC ACTGGGTAACCTG – 3'
ncOGT D152A REV	5' – CAGTACAGGTCCGGGTTG – 3'
ncOGT D114A FOR	5' – GAAAACGGACTTCATC GC AGGTTACATCAACCTGGCTG – 3'
ncOGT D114A REV	5' – CAGCCAGGTTGATGTAACCT GC GATGAAGTCCGGTTTC – 3'
TAB1 S395A FOR	5' – GTGTCTGTGCCATAC GC AAGCGCCCAGAGCACC – 3'
TAB1 S395A REV	5' – GGTGCTCTGGGCGCTT GC GTATGGCACAGACAC – 3'
CAMKIV S189A FOR	5' – CCAAATCGCTGATTTTGGACTC GC AAAAATTGTGGAACATCAAGTGCTC – 3'
CAMKIV S189A REV	5' – GAGCACTTGATGTTCCACAATTTT GC GAGTCCAAAATCAGCGATTTTG – 3'

Table of Gene Blocks

Gene Block ID	Sequence
ncOGT N5A-2 (N186A/N220A/N254A/N288A /N322A) gene block	5' – CGCTGTTGCTTGGTCT GC ACTGGGTTGCGTTTTCAACGCTCAGGGTGAA ATCTGGCTGGCTATCCACCACTTCGAAAAAGCTGTTACCCTGGACCCGAAC TCCTGGACGCTTACATC GC ACTGGGTAACGTTCTGAAAGAAGCTCGTCGTAT CTTCGACCGTGCTGTTGCTGCTTACCTGCGTGCTCTGTCTCTGTCTCCGAAC CACGCTGTTGTTACCGGT GC ACTGGCTTGCCTTTACTACGAACAGGGTCTGA TCGACCTGGCTATCGACACCTACCGTCGTGCTATCGAACTGCAGCCGCACTT TCCAGATGCTTACTG GC ACTGGCTAACGCTCTGAAAAGAAAAAGGTTCTGTT GCTGAAGCTGAAGACTGCTACAACACCGCTCTGCGTCTGTGCCCGACCCAC GCTGACTCTCTGAAC GC ACTGGCTAACATCAAACGTGAAC – 3'
ncOGT N5A-3 (N84A/N118A/N155A/N186A/ N220A) gene block	5' – GCTGGCTGAAGCTTACTCT GC ACTGGGTAACGTTTACAAAGAACG TGGTCAGCTGCAGGAAGCTATCGAACACTACCGTCACGCTCGCGTCT GAAACCGGACTTCATCGACGGTTACATC GC ACTGGCTGCTGCTCTGG TTGCTGCTGGTGACATGGAAGGTGCTGTTTACGGCTTACGTTTCTGCTC TGCAGTACAACCCGGACCTGTACTGCGTTTCTGACCTGGGT GC A CTGCTGAAAGCTCTGGGTCGTCTGGAAGAAGCTAAAGCTTGCTACCT GAAAGCTATCGAAACCCAGCCGAACCTTCGCTGTTGCTTGGTCT GC AC TGGGTTGCGTTTTTCAACGCTCAGGGTGAAATCTGGCTGGCTATCCAC CACTTCGAAAAAGCTGTTACCCTGGACCCGAACCTTCCTGGACGCTTAC ATC GC ACTGGGTAACGTTCTGAAAG – 3'

Construction of pet24-8XHIS-HRV3C-ncOGT variants

All plasmids containing mutations within ncOGT's TPR domain were derived from the pET24b-8XHIS-HRV3C-ncOGT WT parent plasmid using the following methods:

Asparagine ladder variants: Using Gibson Assembly cloning, five sequential asparagine to alanine point mutations were made by inserting a ~450 base pair gene blocks containing the OGT sequences with the specific five sequence asparagine residues mutated to the GCA (alanine) codon. These gene blocks were designed to contain ~15-20 base pair of homology on either end to the site of incorporation in the pET24b-8XHIS-HRV3C-ncOGT WT plasmid. Primers were designed to linearize the pET24b-8XHIS-HRV3C-ncOGT WT plasmid at either side of the given gene block insertion. Each set of primers for a given N5A variant were used to amplify linearized version of the parent plasmid without the region containing the mutations. The amplified PCR products were gel extracted and incubated with the Gibson Assembly Master Mix (NEB) at 50 °C for 1 hour. The assembled plasmids were transformed into STELLAR cloning cells and confirmed by Sanger sequencing.

Aspartate ladder and TPR truncation variants: Using QuickChange site-directed mutagenesis, single point mutations or truncation mutants were made by replacing the existing amino acid in the TPR lumen with the GCA (alanine) codon or deleting specific regions from the TPR domain. PCR primers were designed to have ~15-20 base pairs of homology on either side of the mutation or deletion site. Each set of primers for a given variant

were used to amplify the TPR mutation using the parent plasmid as the template. The amplified PCR products were digested with the Dpn1 restriction enzyme to digest the parent plasmid, leaving the desired mutant plasmids. The digested DNA products were transformed into STELLAR or Nova Blue cloning cells and confirmed by Sanger sequencing.

Construction of TAB1 S395A and CAMKIV S189A variants

Using QuickChange site-directed mutagenesis, single point mutations mutants were made in the pET28a-TAB1 or pET28a-CAMKIV parent plasmids by replacing the existing amino acid with the GCA (alanine) codon. PCR primers were designed to have ~15-20 base pairs of homology on either side of the mutation site. Each set of primers for a given variant were used to amplify the glycosite mutation using the parent plasmid as the template. The amplified PCR products were digested with the Dpn1 restriction enzyme to digest the parent plasmid, leaving the desired mutant plasmids. The digested DNA products were transformed into STELLAR or Nova Blue cloning cells and confirmed by Sanger sequencing.

Bacterial expression and purification of 8XHIS-HRV3C-ncOGT variants

Expression of 8XHIS-HRV3C-ncOGT WT, TPR truncation mutants, and TPR point mutants were carried out in LOBSTR (BL21-DE3) cells (Kerafast). 50 mL starter cultures of 50 µg/mL kanamycin supplemented LB media were grown at 37 °C (250 rpm) from a single colony before addition to 1.5 L of LB media supplemented with 50 µg/mL kanamycin. Cells were grown at 37 °C (250 rpm) to an OD600 of 1.0. The cells were cooled to 16 °C for 30 minutes, and expression was induced with 0.2 mM isopropyl β-D-1-thiogalactopyranoside (IPTG) overnight at 16 °C. The cells were pelleted by centrifugation at 4200 rpm for 20 minutes and stored at -80 °C until lysis.

For protein purifications, the cell pellets lysed via cell disruption and purified using Ni-NTA agarose superflow resin (Qiagen) as previously described.⁹ The eluates were supplemented with 1mM trishydroxypropylphosphine (THP) and concentrated using 100K MWCO Amicon concentration tubes (Millipore) for full-length ncOGT variants and 50K MWCO Amicon concentration tubes for the ncOGT TPR truncation variants. The proteins were isolated through size-exclusion chromatography using a Superdex 200 increase 10/300 GL column (GE Life Sciences) with 1X TBS, pH 7.4. The resulting fractions' identity were verified by SDS-PAGE with appropriate molecular weight standards. Fractions containing the ncOGT variants were pooled and concentrated using the 100K MWCO Amicon concentration tube (50K MWCO tubes for TPR truncations). The concentrated protein was aliquoted and stored at -80 °C until use. Before use, OGT aliquots were thawed on ice, and centrifuged at max speed for 20 minutes at 4 °C to pellet any aggregated protein. The supernatant was removed and store on ice until use, with the concentration measured using A280 with the extinction coefficient of 117580 M⁻¹cm⁻¹ for full-length ncOGT, 77240 M⁻¹cm⁻¹ for OGT 4.5, 80220 M⁻¹cm⁻¹ for OGT 5.5, 84690 M⁻¹cm⁻¹ for OGT 6.5, 82170 M⁻¹cm⁻¹ for OGT 7.5, 93170 M⁻¹cm⁻¹ for OGT 8.0, and 100160 M⁻¹cm⁻¹ for OGT 9.0.

In vitro glycosylation of HeLa extracts by ncOGT variants

Protein glycosylation profiles for each ncOGT variants were determined in HeLa whole cell extracts that were prepared as previously described.⁸ For these experiments, HeLa cell extracts were thawed on ice and centrifuged at 4 °C for 20 minutes at 45,000 rpm (Beckman Coulter TLA120.2 rotor) to pellet any remaining precipitated debris. Following centrifugation, the HeLa cell extracts were aliquoted to a final volume of 40 µL. The aliquots were incubated with 1 mM of UDP-GlcNAc and equal volumes of reaction buffer (20 mM Tris, pH 7.4, 150 mM NaCl, 20 mM MgCl₂, 1 mM THP) and 1 µM OGT for ncOGT D2A and D4A mutants or 2.5 µM OGT for ncOGT N5A mutants at 37 °C. At 1 minute, 5 minutes, and 15 minutes, 10 µL aliquots were taken from the reaction and quenched with 10 µL 2X Laemmli loading buffer containing β-mercaptoethanol. The samples were boiled at 95 °C for 10 minutes and run on a 4-20% TGX SDS-PAGE gel (Bio-Rad) at 180 V for 1.5 hours. The gels were transferred to PVDF membranes (BioRad) and analyzed by western blot with the anti-O-GlcNAc (CTD110.6, Cell Signaling), anti-OGT (D1D8Q, Cell Signaling), and anti-GAPDH (9484, Abcam) antibodies. Activity (densitometry) calculated in ImageJ by measuring the entire lane for each mutant, normalizing to the corresponding WT lane, and using the following equation:
$$\frac{[(\frac{mut\ 1\ min}{wt\ 1\ min}) + (\frac{mut\ 5\ min}{wt\ 5\ min}) + (\frac{mut\ 15\ min}{wt\ 15\ min})]}{3}$$
. Activity reported is an average of two biological replicates.

Bacterial expression and purification of OGT substrates

Expression of pET28a-CARM1, CAMKIV, and TAB1 were carried out in LOBSTR (BL21-DE3) cells (Kerafast). 50 mL starter cultures of 50 µg/mL kanamycin supplemented LB media were grown at 37 °C (250 rpm) from a single colony before addition to 1.5 L of LB media supplemented with 50 µg/mL kanamycin. Cells were grown at 37 °C (250 rpm) to an OD600 of 0.6. The cells were cooled to 16 °C for 30 minutes, and expression was induced with 0.2 mM isopropyl β-D-1-thiogalactopyranoside (IPTG) overnight at 16 °C. The cells were pelleted by centrifugation at 4200 rpm for 20 minutes and stored at -80 °C until lysis.

The cell pellets were resuspended in 1X TBS, pH 7.4 (50 mM Tris, pH 7.4, 150 mM NaCl, supplemented with 0.1 mg/mL lysozyme, 0.1 mg/mL DNase I, and 1 mM PMSF) at 4 °C for 30 minutes. The cells were lysed using an Avestin Emulsiflex C3 cell disruptor (ATA Scientific) three times at 15,000 psi and the debris was pelleted through centrifugation at 14,000xg for 20 minutes at 4 °C. The supernatant was collected, and 40 mM imidazole was added before the lysate was incubated with Ni-NTA agarose superflow resin (Qiagen) for 1 hour at 4 °C, which was prewashed with 3 column volumes 1X TBS, pH 7.4 + 40 mM imidazole for nickel affinity purification. The flow through was removed and the resin was washed with 10 column volumes of 1X TBS, pH 7.4 + 50 mM imidazole. The protein was then eluted with 4 column volumes 1X TBS, pH 7.4 + 250 mM imidazole. The eluate supplemented with 1 mM THP and concentrated using a 30K MWCO Amicon concentration tube (Millipore). The protein was isolated through size-exclusion chromatography using a Superdex 75 increase 10/300 GL column (GE Life Sciences) with 1X TBS, pH 7.4. The resulting fractions' identity were verified by SDS-PAGE with appropriate molecular weight standards. Fractions contains the ncOGT variants were pooled and concentrated using the 30K MWCO Amicon concentration tube. The concentrated protein was aliquoted and stored at -80 °C until use. Before use, OGT aliquots were thawed on ice, and centrifuged at max speed for 20 minutes at 4 °C to pellet any aggregated protein. The supernatant was removed and store on ice until use, with the concentration measured using A280 with the extinction coefficient of 61170 M⁻¹cm⁻¹ for CARM1, 48360 M⁻¹cm⁻¹ for CAMKIV, and 37360 M⁻¹cm⁻¹ for TAB1.

In vitro glycosylation of OGT substrates by ncOGT variants

ncOGT variants and the purified substrates, CARM1, CAMKIV, and TAB1 were thawed on ice, and centrifuged at 4 °C for 20 minutes at max speed (Eppendorf 5424R) to pellet any remaining precipitated debris. Following centrifugation, 2.5 µM OGT, 15 µM substrate, 1 mM UDP-GlcNAc were incubated in reaction buffer (20 mM Tris, pH 7.4, 150 mM NaCl, 20 mM MgCl₂, 1 mM THP) at a final volume of 20 µL for 90 minutes at 37 °C, 350 rpm. The reactions were quenched with 20 µL 2X Laemmli loading buffer containing β-mercaptoethanol. The samples were boiled at 95 °C for 10 minutes and run on a 4-20% TGX SDS-PAGE gel (Bio-Rad) at 180 V for 1.5 hours. The gels were transferred to nitrocellulose membranes and analyzed by western blot with the anti-O-GlcNAc (CTD110.6, Cell Signaling) primary antibody and anti-mouse IgG-680RD IRDye (LI-COR) secondary antibody. Activity (densitometry) reported in Tables S3-5 calculated in ImageJ by measuring the densitometry of substrate glycosylation band for each mutant, normalizing to the corresponding WT lane using the following equation:

$$\frac{\text{Mutant activity}}{\text{WT activity}}. \text{ Activity reported is an average of two replicates.}$$

In vitro turnover assay of TAB1 glycosylation by ncOGT variants

Turnover rates of TAB1 WT and S395A glycosylation for ncOGT WT and D2A-2_{prox} were determined using an *in vitro* glycosylation time course followed by western blotting. For each reaction, 1 µM ncOGT variant, 20 µM TAB1, and 1 mM UDP-GlcNAc were incubated in reaction buffer (20 mM Tris, pH 7.4, 150 mM NaCl, 20 mM MgCl₂, 1 mM THP) at a total volume of 90 µL. Reactions were incubated at 37 °C with 350 rpm shaking. At 0, 1, 2.5, 5, 10, 15, 20, and 30 minutes for TAB1 WT and 0, 1, 5, 10, 15, 20, and 30 minutes for TAB1 S395A, 10 µL of each reaction was removed and quenched with 10 µL 2X Laemmli loading buffer containing β-mercaptoethanol. The samples were boiled at 95 °C for 10 minutes. The samples were split between two 4-20% TGX SDS-PAGE gels (Bio-Rad) and ran at 180V for 1.5 hours. One gel was stained with Pierce ImperialTM protein stain according to the manufacturer's protocol, while the other was transferred to a nitrocellulose membrane and analyzed by western blot with the anti-O-GlcNAc (CTD110.6, Cell Signaling) primary antibody and anti-mouse IgG-680RD IRDye (LI-COR) secondary antibody. Activity (densitometry) reported in Figure 4G and Tables S6-7 was calculated in ImageJ for each timepoint by measuring the densitometry of the full-length glycosylated substrate band. Substrate turnover by ncOGT variants reported in Figure 4G was calculated by fitting the linear ranges of the activity curves and taking the slopes of the resultant lines of best fit. Relative

turnover was calculated using the following equation: $\frac{\text{slope of mutant turnover}}{\text{slope of WT turnover}}$. Data reported is an average of two replicates.

***In vitro* time-dependent glycosylation of CAMKIV by ncOGT variants**

The time dependent of CAMKIV WT and CAMKIV S189A glycosylation by ncOGT WT and D2A-3med were determined using an *in vitro* glycosylation time course followed by western blotting. For each reaction, 2.5 μ M ncOGT variant, 15 μ M CAMKIV variant, and 1 mM UDP-GlcNAc were incubated in reaction buffer (20 mM Tris, pH 7.4, 150 mM NaCl, 20 mM MgCl₂, 1 mM THP) at a total volume of 55 μ L. Reactions were incubated at 37 °C with 350 rpm shaking. At 0, 15, 30, 60, and 90 minutes for CAMKIV WT and 0, 5, 15, 30, and 60 minutes for CAMKIV S189A, 10 μ L of each reaction was removed and quenched with 10 μ L 2X Laemmli loading buffer containing β -mercaptoethanol. The samples were boiled at 95 °C for 10 minutes. The samples were split between two 4-20% TGX SDS-PAGE gels (Bio-Rad) and ran at 180 V for 1.5 hours. One gel was stained using InstantBlue™ protein stain (Sigma-Aldrich) according to the manufacturer's protocol, while the other was transferred to a nitrocellulose membrane and analyzed by western blot using the anti-O-GlcNAc (CTD110.6, Cell Signaling) primary antibody and anti-mouse IgG-680RD IRDye (LI-COR) secondary antibody.

References

1. Jinek, M.; Rehwinkel, J.; Lazarus, B.D.; Izaurralde, E.; Hanover, J.A.; Conti, E., *Nature Structural & Molecular Biology* **2004**, 11(10), 1001.
2. Ashkenazy, H.; Abadi, S.; Martz, E.; Chay, O.; Mayrose, I.; Pupko, T.; Ben-Tal, N., *Nucleic Acids Research* **2016**, 44, W344.
3. Ashkenazy, H.; Erez, E.; Martz, E.; Pupko, T.; Ben-Tal, N. *Nucleic Acids Research* **2010**, 38, W529.
4. Shen, D.L.; Gloster, T.M.; Yuzwa, S.A.; Vocadlo, D.J. *Journal of Biological Chemistry* **2012**, 287(19), 15395.
5. Lazarus, M.B.; Nam, Y.; Jiang, J.; Sliz, P.; Walker, S. *Nature* **2011**, 469(7331), 564.
6. Gross, B.J.; Kraybill, B.C., Walker, S. *J. Am. Chem. Soc.* **2005**, 127(42), 14588.
7. Lazarus, M.B.; Jiang, J.; Kapuria, V.; Bhuiyan, T.; Janetzko, J.; Zandberg, W.F.; Vocadlo, D.J.; Walker, S. *Science* **2013**, 342(6163), 1235.
8. Levine, Z.G.; Fan, C.; Melicher, M.S.; Orman, M.; Benjamin, T.; Walker, S. *J. Am. Chem. Soc.* **2018**, 140(10), 3510.
9. Joiner, C.M.; Levine, Z.G.; Aonbangkhen, C.; Woo, C.M.; Walker, S. *J. Am. Chem. Soc.* **2019**, 141(33), 12974.